RESEARCH AND DEVELOPMENT ON LEAD-BISMUTH TECHNOLOGY FOR ACCELERATOR-DRIVEN TRANSMUTATION SYSTEM AT JAERI

Yuji Kurata[1], **Kenji Kikuchi**[1], **Shigeru Saito**[1],
Kinya Kamata[2], **Teruaki Kitano**[2], **Hiroyuki Oigawa**[1]
[1]Japan Atomic Energy Research Institute, Japan
[2]Mitsui Engineering & Shipbuilding Co., Ltd., Japan

Abstract

R&D on lead-bismuth technology have been conducted for an accelerator-driven system. From the test results of 316SS using JLBL-1 for 3 000 h without active oxygen control, mass transfer from high temperature to low temperature parts was observed. It was found that deposition of Pb/Bi and Fe-Cr grains in the annular channel of the electro-magnetic pump caused plugging and decrease in flow rate. The modification of the loop system brought about a good effect on operation. Significant erosion/ corrosion was not observed in the experiment using the MES loop for 1 000 h under 10^{-5} wt.% oxygen conditions. The results of static corrosion tests showed the following: corrosion depth decreased at 450 C with increasing Cr content in steels while corrosion depth of JPCA and 316SS became larger due to ferritisation caused by dissolution of Ni and Cr at 550 C. Si-added steel exhibited good corrosion resistance at 550 C.

Introduction

The management of high-level radioactive wastes (HLW) is one of the most important issues for the utilisation of nuclear fission energy. The accelerator-driven transmutation system (ADS) is an attractive system which enables to incinerate long-lived nuclear wastes such as minor actinides by combining a proton accelerator, spallation target and subcritical core [1,2]. Therefore, research and development (R&D) concerning the ADS have been carried out in recent years.

Liquid Pb-Bi eutectic (LBE) is a potential candidate of the target and coolant for the ADS. The LBE has the advantage of a low melting point, low vapour pressure, good neutron yield, low neutron absorption and chemical stability in comparison with sodium. However, LBE technologies have not yet been fully established for nuclear systems. In particular, corrosion of structural materials is a concern due to the high solubility of the main elements of the structural materials in LBE.

In order to realise the ADS, JAERI has started a wide range of R&D activities: design study of a large-scale ADS, superconducting linear accelerator, LBE and subcritical reactor physics technologies. In the LBE technologies, four main fields are being studied: 1) corrosion of structural materials, 2) thermal-hydraulics of LBE, 3) behaviour of radioactive impurities, and 4) irradiation damage of materials by protons and neutrons. R&D activities on corrosion of structural materials are reviewed in this paper.

Liquid metal loops are often used to estimate the actual corrosion behaviour in LBE since velocity effect, erosion and mass transfer caused by solution at high-temperature parts and precipitation at low-temperature parts are involved in the ADS plant. The LBE loop for material corrosion (JLBL-1) was installed at JAERI in January 2001 and corrosion tests have been conducted [3,4]. Furthermore, material corrosion loop tests are underway at Mitsui Engineering & Shipbuilding Co., Ltd. (MES) as a joint research to accumulate a materials database for the ADS. Static corrosion tests are also useful for understanding corrosion mechanisms and screening various materials. The purpose of this paper is to describe the status and results of LBE loop tests and static corrosion tests. First, the design of a large-scale ADS will be shortly introduced. After results of material corrosion tests using JLBL-1 are described, the results obtained in an oxygen-controlled LBE using the MES loop are discussed. In addition, static corrosion test results are presented focusing on the effects of temperature and alloying elements in steels on corrosion behaviour.

Design of a large-scale ADS

The ADS proposed by JAERI is an 800 MWth, LBE-cooled, tank-type subcritical reactor with a spallation target of LBE. Figure 1 shows a conceptual drawing of the 800 MWth LBE-cooled ADS. Two criteria were set regarding the thermal-hydraulics and the beam window: 1) the flow rate of LBE should not exceed 2 m/sec and 2) the outer surface temperature of the beam window should not exceed 520 C. As a result of some design modifications, the coolant inlet temperature and outlet temperature were 300 C and 410 C, respectively. Figure 2 shows the results of thermal-hydraulics and temperature analyses for the LBE target and beam window.

Corrosion tests using JLBL-1

Figure 3 shows an initial flow diagram of JAERI materials testing of the Pb-Bi loop (JLBL-1). This loop consists of an electro-magnetic pump, a heater, a test section, a cooler, an expansion tank, an electro-magnetic flow meter and a dump tank. The electro-magnetic pump is a linear inductive type with

Figure 1. Concept drawing of 800 MWth ADS

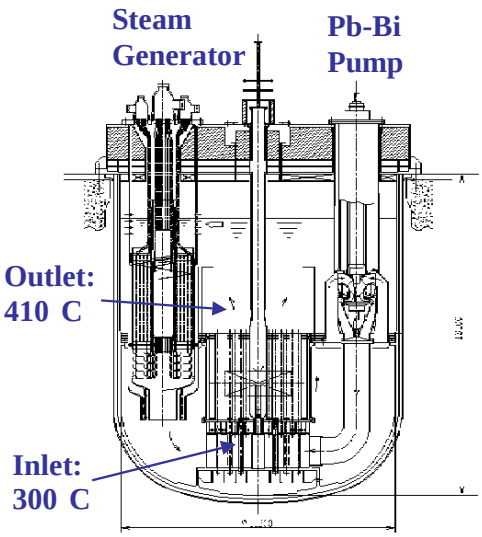

Figure 2. Results of (a) hydraulic and (b) temperature analysis for LBE target and beam window

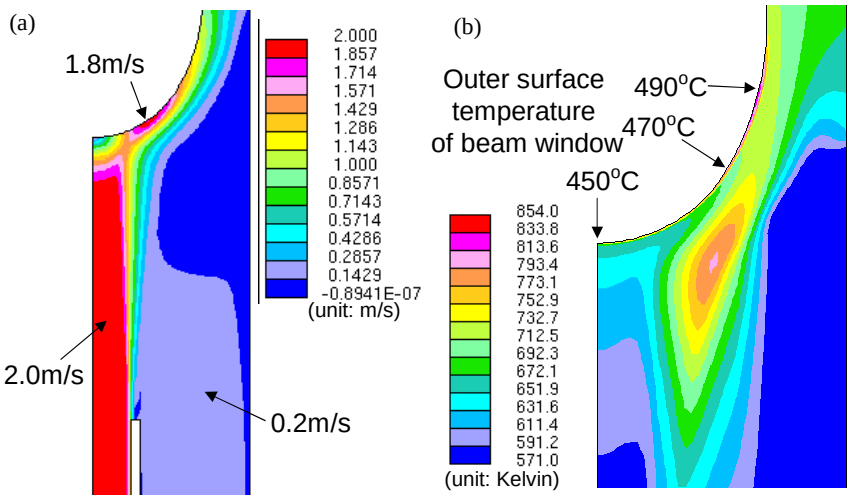

Figure 3. Flow diagram of materials testing Pb-Bi loop (JLBL-1)

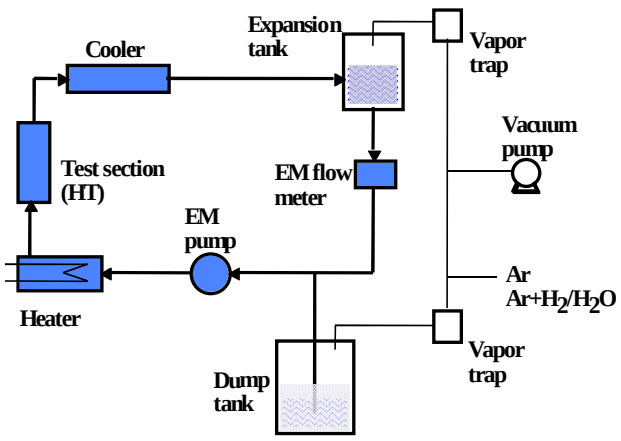

an annular channel. The test section is a specimen tube with an inner diameter of 9.8 mm and a tube thickness of 2 mm. All of the materials for the piping and tanks in contact with LBE were type 316SS. In the first and second tests, type 316SS was used as a specimen tube. During the first test, the maximum temperature, the temperature difference and the flow velocity at the test section were 450 C, 50 C and about 1 m/s, respectively. Initially the electro-magnetic flow meter was calibrated. The calibration curve was obtained from the correlation between the EMF output and the flow rate measured from the time in a constant level change in the expansion tank during the drainage. Figure 4 shows a schematic diagram of the electro-magnetic flow meter and the calibration curve obtained at 400 C. Electrodes of the electro-magnetic flow meter contact with flowing Pb-Bi in the flow channel. As shown in Figure 4, a linear relationship between the output and the flow rate was obtained. An argon gas of 99.95% purity covered the expansion tank during the operation. Oxygen in LBE was not controlled actively. Thin floating oxide was observed on the surface of LBE in the expansion tank through the observing window. It was thus considered that the oxygen concentration under operation was the saturation concentration, $3.2 \cdot 10^{-4}$ wt.%.

Figure 4. Schematic diagram of an electromagnetic flow meter and the relationship between flow rate and the output of the flow meter. The temperature of liquid Pb-Bi was 400 C.

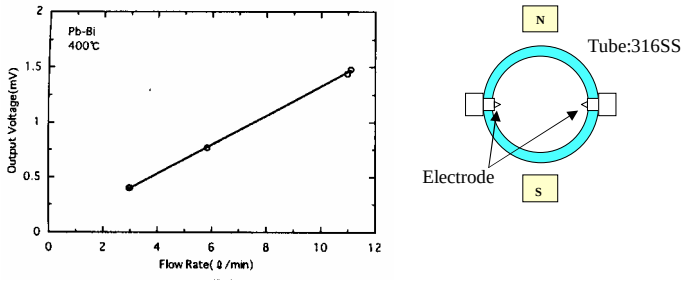

The first test result of JLBL-1 is described hereafter. After the first test of about 3 000 h (3 126 h), a specimen, circulation tubes and an electro-magnetic pump channel were cut and inspected. Figure 5 shows the axial cross-section of type 316SS specimen tube after the corrosion test. As can be seen in this figure, pits and hollows are observed and a grain boundary fissure is also recognised. The final treatment of the type 316SS specimen tube was cleaning with hot acid. Since this treatment produced deeply dug grain boundaries, it is considered that the rough surface with deeply dug grain boundaries accelerated corrosion/erosion by flowing Pb-Bi. The corrosion depth of type 316SS at the high-temperature part is estimated to be about 100 ㎜/3 000 h.

Figure 5. Corrosion of type 316SS tube specimen after the first corrosion test in liquid Pb-Bi using JLBL-1

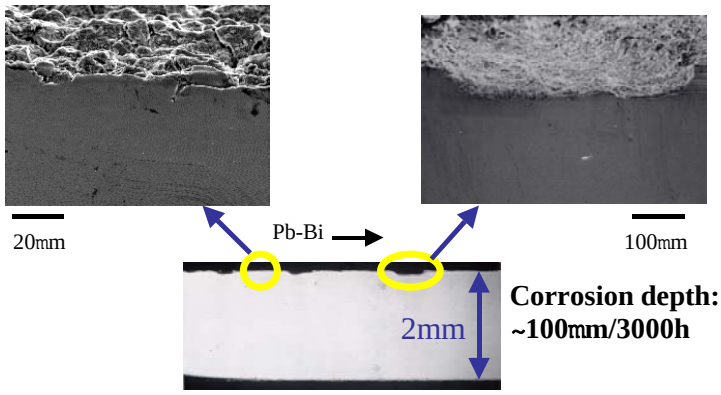

A decrease in the flow rate with increasing operation time was experienced during the first test. It was remarkable when the corrosion test was restarted after draining of Pb-Bi on account of a stoppage of electric supply. In order to examine the cause of the decrease in flow rate, not only a specimen but also circulation tubes and an electro-magnetic pump channel were inspected. Figure 6 shows an appearance of the shaft of the electro-magnetic pump and the analysis of the deposits in a channel. It was found that grey, thick deposits formed in the narrow channel causing plugging and the decrease in flow rate. As shown in Figure 10, the deposits consist of Pb/Bi and grains of Fe-Cr ferrite. Precipitation of these grains consisting of Fe-Cr (Fe:Cr = 9:1) was widely found on the circulation tubes at 400 C [3]. The considered process of dissolution and precipitation is the following: Fe, Cr and Ni are dissolved into Pb-Bi from type 316SS at the high-temperature parts and Fe-Cr grains precipitate at the low-temperature parts according to the difference in solubility.

Figure 6. Analysis of deposits in a narrow channel of the electro-magnetic system: EDX analysis of cross-section of deposits

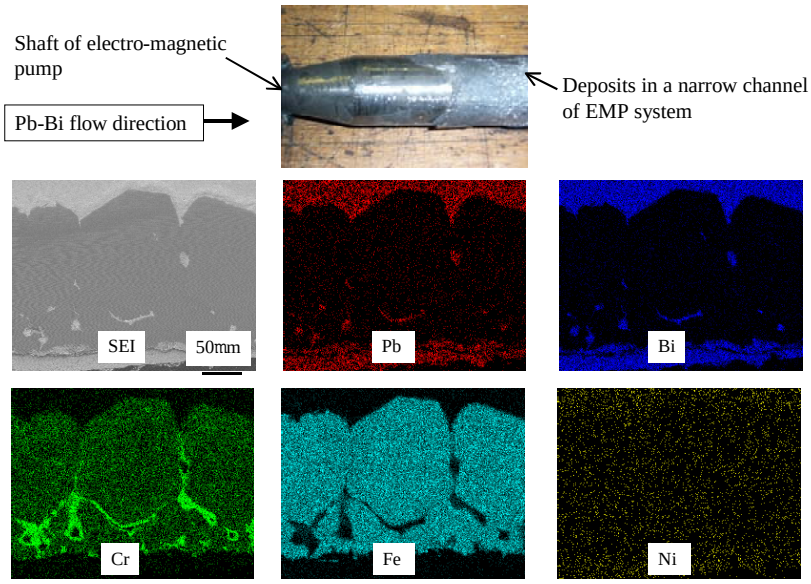

In the second corrosion test, modification of JLBL-1 and the tube specimen was carried out. Three metallic filters were set and the channel of liquid Pb-Bi in the EMP system was made wider in JLBL-1. Although an oxygen control system and an oxygen sensor were also set in the loop, they were not used in the second corrosion test. The inner surface of type 316SS tube specimen was mechanically polished before testing. Other experimental conditions in the second corrosion test were the same as those in the first one. Decrease in Pb-Bi flow was not observed up to 3 000 h in the second test. It is considered that addition of metallic filters to JLBL-1 and modification of the EMP system had a positive effect on the operation of the Pb-Bi loop system. Furthermore, the corrosion depth of type 316SS was reduced to about 20 ㎜ in the second loop test.

Corrosion tests using MES loop

A material corrosion test was conducted using an MES loop to accumulate a wide range of corrosion data in LBE. Figure 7 shows a flow diagram of the MES loop. The loop consists of an electro-magnetic pump, an electro-magnetic flow meter, an economiser, a heater, a test section, an air cooler, an expansion tank, oxygen sensors, an oxygen control system, filters and a dump tank. Oxygen sensors produced by MES were set in the loop. Yttria-stabilised zirconia (YSZ) solid electrolyte and a

Figure 7. Flow diagram of the Mitsui Engineering and Shipbuilding Co., Ltd (MES) loop

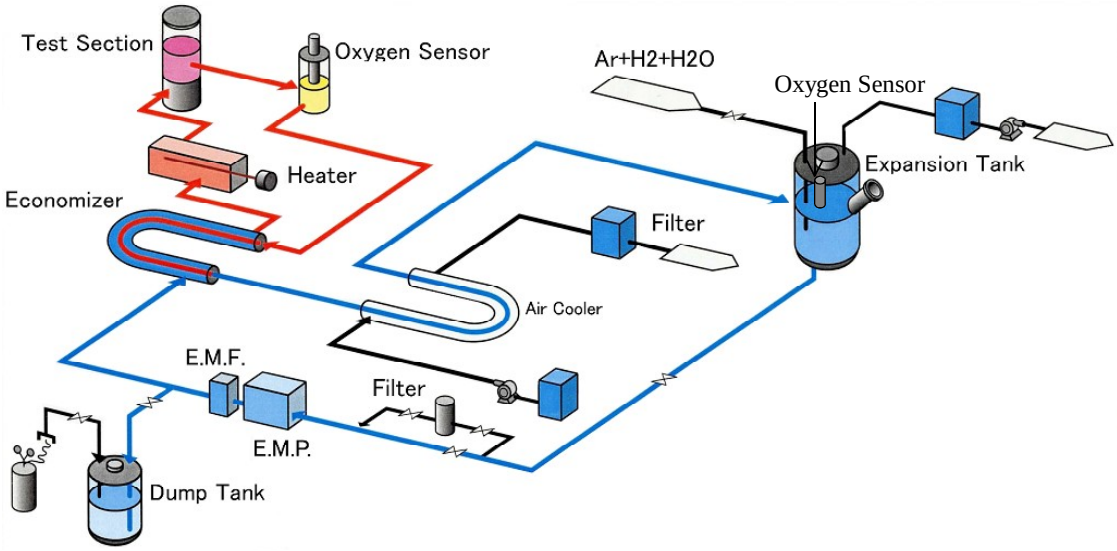

Bi/Bi_2O_3 reference electrode were used in the oxygen sensor. Bubbling of Ar-H_2 gas and Ar-H_2/H_2O gas was used for the control of oxygen concentration in LBE. Figure 8 shows the arrangement of specimens and Pb-Bi flow direction at the test section in MES loop. The relationship between the specimen and the Pb-Bi flow simulated that between the beam duct and Pb-Bi flow in the conceptual drawing of the ADS. The liquid Pb-Bi collides the tip of specimens and flows up the side of specimens axially. The specimen was rod-type with a diameter of 8 mm and a length of 130 mm. JPCA (15Cr-15Ni-2Mo) and F82H (8Cr-2W) steels were used as specimens. During the test using the MES loop, the maximum temperature, temperature difference and flow velocity at the test section inlet were 450 C, 100 C and 0.4~0.6 m/s, respectively. Oxygen concentration in LBE was controlled to $1 \cdot 10^{-5}$ wt%. The test time was 1 000 h.

Figure 8. Schematic drawing of test section in the MES loop and rod-type corrosion specimens

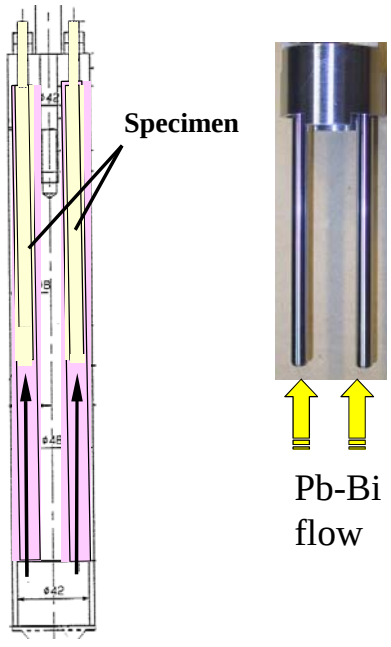

Figure 9 shows a cross-section of the F82H specimen after corrosion for 1 000 h. Significant corrosion/erosion was not observed at either the tip or side parts at 450 C for 1 000 h. Uniform oxide films were formed on the surface of all parts including the tip. From electron-probe micro analysis and X-ray diffraction results, the oxide films consist of outer magnetite, Fe_3O_4 and inner spinel Fe-Cr oxide. The thickness of the oxide films was from 6 to 8 mm. The thickness of the oxides formed on F82H in this study was below half that formed on 2.25Cr-1Mo steel tested under similar conditions at the Institute for Physics and Power Engineering (IPPE) loop. As seen in Figure 10, no significant corrosion/erosion was observed for the JPCA specimen, although there were small hollows with a depth of 1~2 mm near the corner of the tip. A hole with a depth of 8~10 mm was also observed near the corner of JPCA (Figure 11). The oxide film was not detected on the surface of the JPCA specimen by usual methods. A corrosion test with a maximum temperature of 500 C is underway using the MES loop. Corrosion tests with longer times are also scheduled.

Figure 9. Cross-section of F82H specimen after corrosion test for 1 000 h using the MES loop

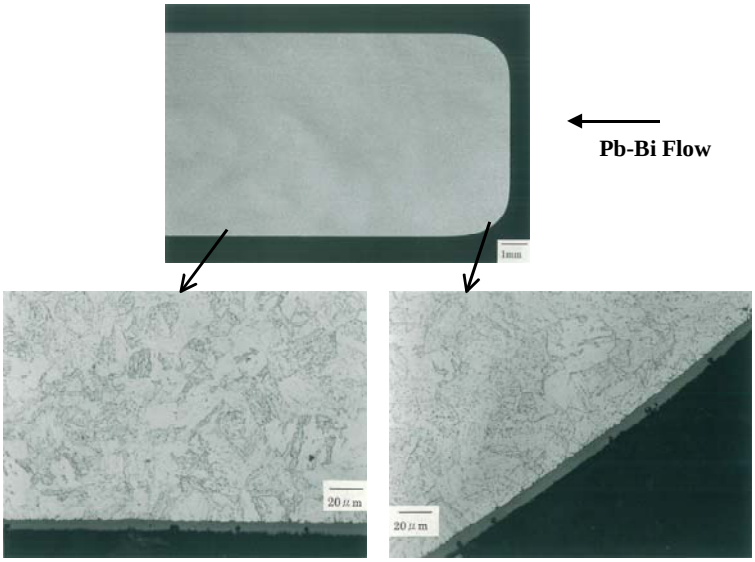

Figure 10. Cross-section of JPCA specimen after corrosion test for 1 000 h using the MES loop

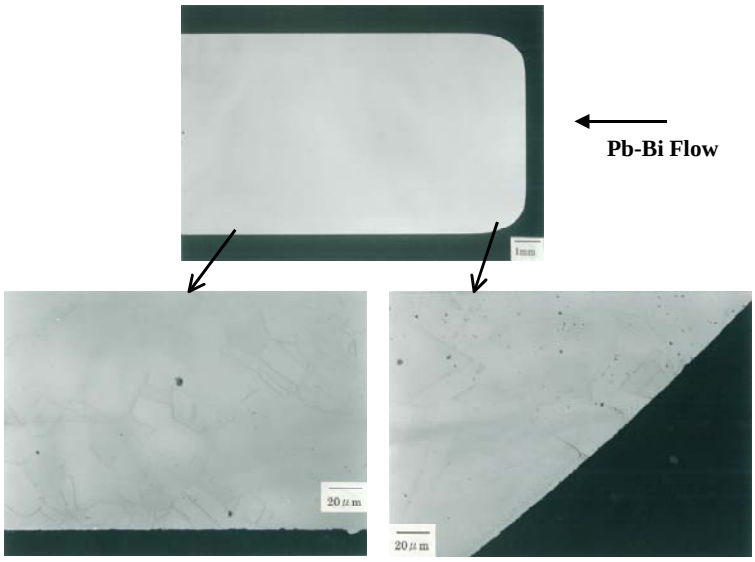

Figure 11. A hole with a depth of 8~10㎛m observed on the corner at JPCA specimen after corrosion test

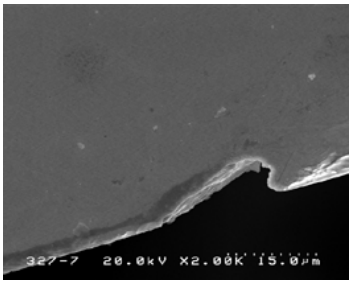

Static corrosion tests

Static corrosion tests of various steels were conducted in oxygen-saturated liquid Pb-Bi at 450 C and 550 C for 3 000 h to study the effects of temperature and alloying elements on corrosion behaviour. Materials used in the experiment were F82H (8Cr-2W), Mod.9Cr-1Mo (9Cr-1Mo), 410SS (12Cr), 430SS (16Cr), 2.25Cr-1Mo, Fe, JPCA (15Cr-15Ni), 316SS (17Cr-11Ni) steels and Si-added steel, SX (18Cr-19Ni-5Si). The size of corrosion specimens was 15 mm · 30 mm · 2 mm, and a hole 7.2 mm in diameter was made at the top of the specimen for installation. Figure 12 shows a schematic drawing of static corrosion equipment. Components contacting liquid Pb-Bi were made of quartz in the corrosion equipment. Fresh eutectic Pb-Bi (45Pb-55Bi) of 7 kg was used in the test. The Pb-Bi was melted in a pot under an argon gas environment. Argon gas of 99.9999% purity was used as a cover gas over the liquid Pb-Bi. Corrosion tests were conducted at 450 C and 550 C for 3 000 h. A thin PbO film was formed on the surface of the liquid Pb-Bi and corrosion tests were made in oxygen-saturated liquid Pb-Bi. Oxygen saturation concentration was estimated to be $3.2 \cdot 10^{-4}$ wt.% at 450 C and $1.2 \cdot 10^{-3}$ wt.% at 550 C using the equation in the literature [5].

Figure 12. Schematic drawing of static corrosion equipment in liquid Pb-Bi

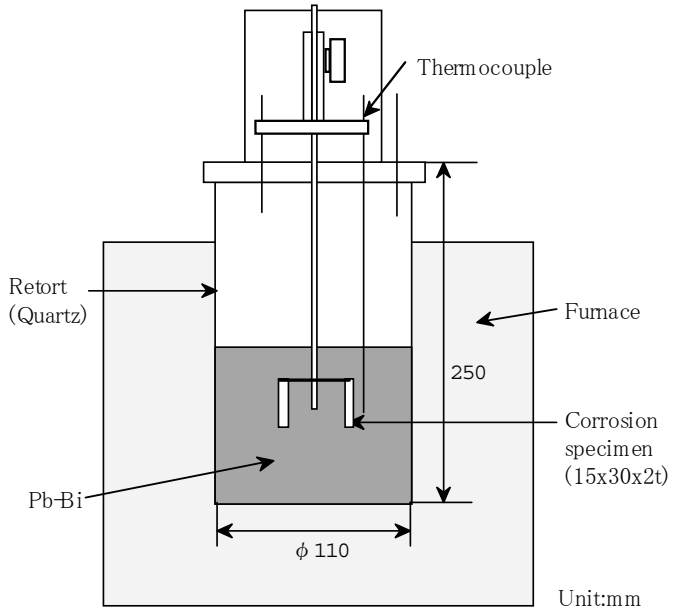

Figure 13 shows the relationship between corrosion depth and Cr content in steels with some scanning electron microscope (SEM) images after corrosion at 450 C. Corrosion depth decreased at 450 C with increasing Cr content in the steels regardless of ferritic/martensitic steels or austenitic steels. The corrosion depth of Si-added steel, SX, was very small. The corrosion films of the steels, except for SX, were oxides of Fe and Cr. A decrease in Cr, Ni and Fe concentrations was not observed near the surface region from the results of EDX analysis for JPCA and 316SS specimens after corrosion at 450 C; it is considered that appreciable dissolution of these elements has not occurred under these conditions.

Figure 13. Results of static corrosion test at 450 C for 3 000 h

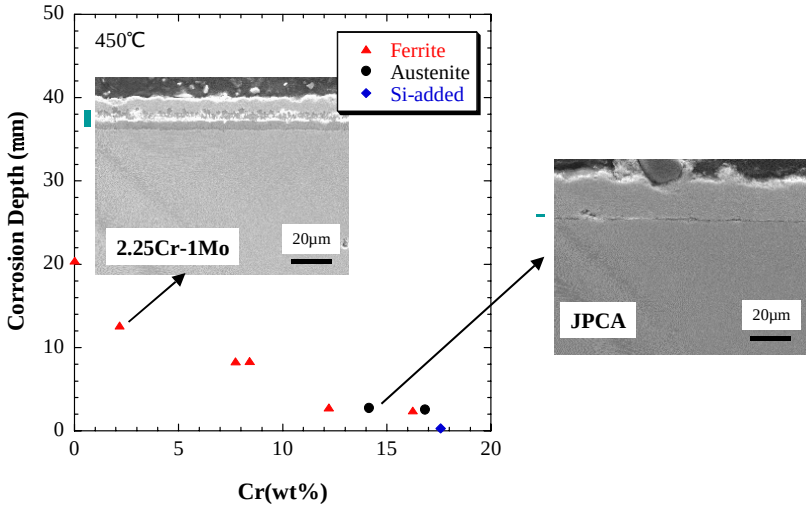

On the other hand, the thick ferrite layer produced by dissolution of Ni and Cr was formed on the surface of JPCA and type 316SS with low Si contents. Pb and Bi penetrated into the formed ferrite layer. Figure 14 shows the relationship between corrosion depth and Cr content in steels with some SEM images after corrosion at 550 C. The corrosion depth of ferritic/martensitic steels, which is shown as a triangle in the figure, also decreases at 550 C with increasing Cr content in the steels while corrosion depth of austenitic steels, JPCA and 316SS, becomes large because of the formation of the ferrite layer at 550 C.

Figure 14. Results of static corrosion test at 550 C for 3 000 h

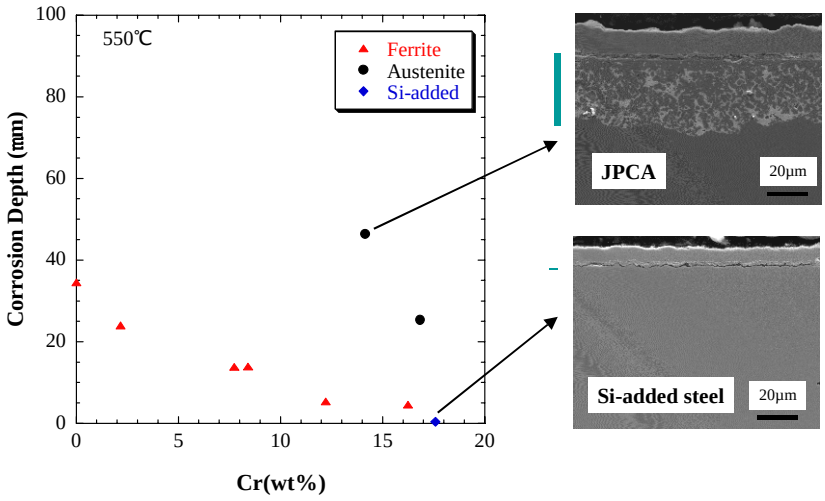

The corrosion depth of SX is very small at 550 C in spite of the austenitic steel. A protective oxide film composed of Si and O is formed on the surface of SX containing 4.8% Si during corrosion in liquid Pb-Bi at 550 C. The thin oxide film prevents dissolution of Ni and Cr into Pb-Bi and the steel containing Si shows excellent corrosion resistance in LBE [6]. Martensitic steels containing Si were developed for nuclear use in Russia [7]. Russian martensitic steel with 1.8% Si exhibited good corrosion resistance in flowing liquid Pb-Bi [8,9]. Some Al surface-alloyed steels also showed good corrosion resistance in flowing liquid Pb-Bi [10]. It is considered that SX steel exhibited good corrosion resistance in LBE because of its high Si content, about 5%.

Conclusions

Research and development on lead-bismuth technology for ADS have been conducted at JAERI and MES as a joint research programme with progress of design study of a large-scale ADS. The main results are as follows:

- From the first test result of JLBL-1, mass transfer from high-temperature to low-temperature parts was observed. Grains of Fe-Cr precipitated at the low-temperature parts. The corrosion depth of type 316SS at the high-temperature part was estimated to be about 100 ㎜/3 000 h. From experience of operating JLBL-1, it was found that deposition of Pb-Bi and Fe-Cr grains in the annular channel of the electro-magnetic pump caused plugging and decrease in flow rate. The modification of the loop system such as adoption of metallic filters and a wide channel, and the use of an inner-polished 316SS tube brought about a good effect.

- The corrosion test using the MES loop was conducted under the condition where the liquid Pb-Bi collides with the tip of rod-type specimens under oxygen-controlled conditions. Significant corrosion/erosion was also not observed for F82H and JPCA specimens in the experiment for 1 000 h under 10^{-5} wt.% oxygen condition. Oxygen control techniques in LBE were obtained through operating the MES loop.

- The results of static corrosion tests under oxygen-saturated conditions showed effects of temperature and alloying elements in steels on corrosion behaviour. Corrosion depth decreased at 450 C with increasing Cr content in steels regardless of ferritic/martensitic steels or austenitic steels. The corrosion depth of ferritic/martensitic steels also decreased at 550 C with increasing Cr content in steels, whereas the corrosion depth of austenitic steels, JPCA and 316SS became larger due to ferritisation caused by dissolution of Ni and Cr at 550 C than that of ferritic/ martensitic steels. An austenitic stainless steel containing about 5% Si exhibited fine corrosion resistance at 550 C because the protective Si oxide film was formed.

Acknowledgements

This work was partly funded by the Ministry of Education, Culture, Sports, Science and Technology (MEXT) as one of the R&D programmes for innovative nuclear systems. The authors are grateful to Drs. Tsujimoro, Sasa and Nishihara of JAERI, Dr. Iwata of Mitsubisi Heavy Industries Ltd and Dr. Ono of Mitsui Engineering & Shipbuilding Co., Ltd.

REFERENCES

[1] Takano, H., K. Nishihara, K. Tsujimoto, T. Sasa, H. Oigawa and T. Takizuka, *Progress in Nuclear Energy*, 37, 371 (2001).

[2] Mukaiyama, T., T. Takizuka, M. Mizumoto, Y. Ikeda, T. Ogawa, A. Hasegawa, H. Takada and H. Takano, *Progress in Nuclear Energy*, 38, 107 (2001).

[3] Kikuchi, K., Y. Kurata, S. Saito, M. Futakawa, T. Sasa, H. Oigawa, E. Wakai, K. Miura, *J. Nucl. Mater*., 308, 348 (2003).

[4] Kurata, Y., M. Futakawa, K. Kikuchi, S. Saito, T. Osugi, *J. Nucl. Mater*., 301, 28 (2002).

[5] Gromov, B.F., Y.I. Orlov, P.N. Martynov and V.A. Gulevsky, *Proceedings of Heavy Liquid Metal Coolants in Nuclear Technology, HLMC'98*, 5-9 October 1998, Obninsk, Russia, p. 87 (1999).

[6] Kurata, Y., M. Futakawa, *J. Nucl. Mater*., 325, 217 (2004).

[7] Yachmenyov, G.S., A.Ye. Rusanov, B.F. Gromov, Yu.S. Belomytsev, N.S. Skvortsov and A.P. Demishonkov, *Proceedings of Heavy Liquid Metal Coolants in Nuclear Technology, HLMC'98*, 5-9 October 1998, Obninsk, Russia, p. 133 (1999).

[8] Barbier, F., A. Rusanov, *J. Nucl. Mater*., 296, 231 (2001).

[9] Benamati, G., C. Fazio, H. Piankova, A. Rusanov, *J. Nucl. Mater*., 301, 23 (2002).

[10] Mueller, G., A. Heinzel, J. Konys, G. Schumacher, A. Weisenburger, F. Zimmermann V. Engeliko, A. Rusanov, V. Markov, *J. Nucl. Mater*., 301, 40 (2002).

TABLE OF CONTENTS